Biomedical Optics EXPRESS

# Laser induced breakdown spectroscopy for bone and cartilage differentiation - ex vivo study as a prospect for a laser surgery feedback mechanism

**Fanuel Mehari,[1,2*] Maximilian Rohde,[3] Christian Knipfer,[3] Rajesh Kanawade,[1,2] Florian Klämpfl,[1, 2] Werner Adler,[4] Florian Stelzle,[1,3] and Michael Schmidt[1,2]**

[1]*Clinical Photonics Lab, Erlangen Graduate School in Advanced Optical Technologies (SAOT), Friedrich-Alexander-Universität Erlangen-Nürnberg, Paul-Gordan-Strasse 6, 91052 Erlangen, Germany*
[2]*Institute of Photonic Technologies, Friedrich-Alexander-Universität Erlangen-Nürnberg, Konrad-Zuse-Straße 3/5, 91052 Erlangen, Germany*
[3] *Department of Oral and Maxillofacial Surgery, University Hospital Erlangen, Friedrich-Alexander-Universität Erlangen-Nürnberg, Glückstrasse 11, 91054 Erlangen, Germany*
[4] *Chair of Biometry and Epidemiology, Friedrich-Alexander-Universität Erlangen-Nürnberg, Waldstraße 6, 91054 Erlangen, Germany*
[*]*fanuel.mehari@lpt.uni-erlangen.de*

**Abstract:** Laser surgery enables for very accurate, fast and clean modeling of tissue. The specific and controlled cutting and ablation of tissue, however, remains a central challenge in the field of clinical laser applications. The lack of information on what kind of tissue is being ablated at the bottom of the cut may lead to iatrogenic damage of structures that were meant to be preserved. One such example is the shaping or removal of diseased cartilaginous and bone tissue in the temporomandibular joint (TMJ). Diseases of the TMJ can induce deformation and perforation of the cartilaginous discus articularis, as well as alterations to the cartilaginous surface of the condyle or even the bone itself. This may result in restrictions of movement and pain. The aim of a surgical intervention ranges from specific ablation and shaping of diseased cartilage, bone or synovial tissues to extensive removal of TMJ structures. One approach to differentiate between these tissues is to use Laser Induced Breakdown Spectroscopy (LIBS). The ultimate goal is a LIBS guided feedback control system for surgical laser systems that enables real-time tissue identification for tissue specific ablation. In the presented study, the authors focused on the LIBS based differentiation between cartilage tissue and cortical bone tissue using an ex-vivo pig model.

©2014 Optical Society of America

**OCIS codes:** (170.1020) Ablation of tissue; (170.1470) Blood or tissue constituent monitoring; (170.6935) Tissue characterization; (300.6365) Spectroscopy, laser induced breakdown.

## References and links

1. S. F. Dworkin, K. H. Huggins, L. LeResche, M. Von Korff, J. Howard, E. Truelove, and E. Sommers, "Epidemiology of signs and symptoms in temporomandibular disorders: clinical signs in cases and controls," J. Am. Dent. Assoc. **120**(3), 273–281 (1990).
2. J. A. McNamara, Jr., D. A. Seligman, and J. P. Okeson, "Occlusion, Orthodontic treatment, and temporomandibular disorders: a review," J. Orofac. Pain **9**(1), 73–90 (1995).
3. S. Weedon, N. Ahmed, and A. J. Sidebottom, "Prospective assessment of outcomes following disposable arthroscopy of the temporomandibular joint," Br. J. Oral Maxillofac. Surg. **51**(7), 625–629 (2013).
4. F. Liu and A. Steinkeler, "Epidemiology, Diagnosis, and Treatment of Temporomandibular Disorders," Dent. Clin. North Am. **57**(3), 465–479 (2013).
5. M. F. Dolwick and G. Dimitroulis, "Is there a role for temporomandibular joint surgery?" Br. J. Oral Maxillofac. Surg. **32**(5), 307–313 (1994).
6. G. Dimitroulis, "Temporomandibular joint surgery: what does it mean to the dental practitioner?" Aust. Dent. J. **56**(3), 257–264 (2011).
7. M. G. Koslin, A. T. Indresano, and L. G. Mercuri, "Temporomandibular joint surgery," J. Oral Maxillofac. Surg. **70**(11 Suppl 3), e204–e231 (2012).

#223215 - $15.00 USD Received 15 Sep 2014; revised 16 Oct 2014; accepted 16 Oct 2014; published 21 Oct 2014

8. G. Dimitroulis, "The role of surgery in the management of disorders of the temporomandibular joint: a critical review of the literature. Part 2," Int. J. Oral Maxillofac. Surg. **34**(3), 231–237 (2005).
9. G. Dimitroulis, "The role of surgery in the management of disorders of the Temporomandibular Joint: a critical review of the literature. Part 1," Int. J. Oral Maxillofac. Surg. **34**(2), 107–113 (2005).
10. B. Spyropoulos, "50 years LASERS: in vitro diagnostics, clinical applications and perspectives," Clin. Lab. **57**(3-4), 131–142 (2011).
11. M. Ben-Bassat, I. Kaplan, Y. Shindel, and A. Edlan, "The CO2 laser in surgery of the tongue," Br. J. Plast. Surg. **31**(2), 155–156 (1978).
12. M. S. Strong, C. W. Vaughan, G. B. Healy, S. M. Shapshay, and G. J. Jako, "Transoral management of localized carcinoma of the oral cavity using the CO2 laser," Laryngoscope **89**(6 Pt 1), 897–905 (1979).
13. J. A. Carruth, "Resection of the tongue with the carbon dioxide laser," J. Laryngol. Otol. **96**(6), 529–543 (1982).
14. L. Gáspár, "The use of high-power lasers in oral surgery," J. Clin. Laser Med. Surg. **12**(5), 281–285 (1994).
15. M. L. Schoelch, N. Sekandari, J. A. Regezi, and S. Silverman, Jr., "Laser management of oral leukoplakias: a follow-up study of 70 patients," Laryngoscope **109**(6), 949–953 (1999).
16. J. A. Carruth, "Lasers in medicine and surgery," J. Med. Eng. Technol. **8**(4), 161–167 (1984).
17. M. K. Basu, J. W. Frame, and P. H. Rhys Evans, "Wound healing following partial glossectomy using the $CO_2$ laser, diathermy and scalpel: a histological study in rats," J. Laryngol. Otol. **102**(4), 322–327 (1988).
18. M. Luomanen, "A comparative study of healing of laser and scalpel incision wounds in rat oral mucosa," Scand. J. Dent. Res. **95**(1), 65–73 (1987).
19. S. E. Fisher and J. W. Frame, "The effects of the carbon dioxide surgical laser on oral tissues," Br. J. Oral Maxillofac. Surg. **22**(6), 414–425 (1984).
20. G. L. Bryant, J. M. Davidson, R. H. Ossoff, C. G. Garrett, and L. Reinisch, "Histologic study of oral mucosa wound healing: a comparison of a 6.0- to 6.8-micrometer pulsed laser and a carbon dioxide laser," Laryngoscope **108**(1), 13–17 (1998).
21. P. López-Jornet and F. Camacho-Alonso, "Comparison of pain and swelling after removal of oral leukoplakia with $CO_2$ laser and cold knife: a randomized clinical trial," Med. Oral Patol. Oral Cir. Bucal **18**(1), e38–e44 (2013).
22. A. Pourzarandian, H. Watanabe, A. Aoki, S. Ichinose, K. M. Sasaki, H. Nitta, and I. Ishikawa, "Histological and TEM examination of early stages of bone healing after Er:YAG laser irradiation," Photomed. Laser Surg. **22**(4), 342–350 (2004).
23. M. Ohnishi, "Arthroscopic laser surgery and suturing for temporomandibular joint disorders: technique and clinical results," Arthroscopy **7**(2), 212–220 (1991).
24. M. G. Koslin and J. C. Martin, "The use of the holmium laser for temporomandibular joint arthroscopic surgery," J. Oral Maxillofac. Surg. **51**(2), 122–123 (1993).
25. G. D. Baxter, D. M. Walsh, J. M. Allen, A. S. Lowe, and A. J. Bell, "Effects of low intensity infrared laser irradiation upon conduction in the human median nerve in vivo," Exp. Physiol. **79**(2), 227–234 (1994).
26. T. Menovsky, M. van den Bergh Weerman, and J. F. Beek, "Effect of CO2 milliwatt laser on peripheral nerves: Part I. A dose-response study," Microsurgery **17**(10), 562–567 (1996).
27. T. Menovsky, M. Van Den Bergh Weerman, and J. F. Beek, "Effect of CO(2)-Milliwatt laser on peripheral nerves: part II. A histological and functional study," Microsurgery **20**(3), 150–155 (2000).
28. R. Orchardson, J. M. Peacock, and C. J. Whitters, "Effect of pulsed Nd:YAG laser radiation on action potential conduction in isolated mammalian spinal nerves," Lasers Surg. Med. **21**(2), 142–148 (1997).
29. R. Kanawade, F. Mehari, C. Knipfer, M. Rohde, K. Tangermann-Gerk, M. Schmidt, and F. Stelzle, "Pilot study of laser induced breakdown spectroscopy for tissue differentiation by monitoring the plume created during laser surgery — An approach on a feedback Laser control mechanism," Spectrochim. Acta, B At. Spectrosc. **87**(0), 175–181 (2013).
30. F. Stelzle, C. Knipfer, W. Adler, M. Rohde, N. Oetter, E. Nkenke, M. Schmidt, and K. Tangermann-Gerk, "Tissue Discrimination by Uncorrected Autofluorescence Spectra: A Proof-of-Principle Study for Tissue-Specific Laser Surgery," Sensors (Basel) **13**(10), 13717–13731 (2013).
31. F. Stelzle, I. Terwey, C. Knipfer, W. Adler, K. Tangermann-Gerk, E. Nkenke, and M. Schmidt, "The impact of laser ablation on optical soft tissue differentiation for tissue specific laser surgery-an experimental ex vivo study," J. Transl. Med. **10**, 123 (2012).
32. R. Kanawade, F. Mahari, F. Klämpfl, M. Rohde, C. Knipfer, K. Tangermann-Gerk, W. Adler, M. Schmidt, and F. Stelzle, "Qualitative tissue differentiation by analysing the intensity ratios of atomic emission lines using laser induced breakdown spectroscopy (LIBS): prospects for a feedback mechanism for surgical laser systems," J. Biophotonics 1-9 (2013).
33. D. L. J. R. Dr David A. Cremers, *Handbook of Laser-Induced Breakdown Spectroscopy* (Wiley, 2006)
34. D. A. Cremers and R. C. Chinni, "Laser-Induced Breakdown Spectroscopy - Capabilities and Limitations," Appl. Spectrosc. Rev. **44**(6), 457–506 (2009).
35. A. K. Myakalwar, S. Sreedhar, I. Barman, N. C. Dingari, S. Venugopal Rao, P. Prem Kiran, S. P. Tewari, and G. Manoj Kumar, "Laser-induced breakdown spectroscopy-based investigation and classification of pharmaceutical tablets using multivariate chemometric analysis," Talanta **87**(0), 53–59 (2011).
36. O. Samek, M. Liska, J. Kaiser, V. Krzyzanek, D. C. S. Beddows, A. Belenkevitch, G. W. Morris, and H. H. Telle, "Laser ablation for mineral analysis in the human body: integration of LIFS with LIBS," Biomedical Sensors, Fibers, and Optical Delivery Systems pp. 263–271, SPIE, Stockholm, Sweden (1999).
37. A. Kramida, Y. Ralchenko, and J. Reader, "Team (2012). NIST Atomic Spectra Database (ver. 5.0)," National Institute of Standards and Technology, Gaithersburg, MD (Available at: http://physics.nist.gov/asd)
38. H. Q. Woodard and D. R. White, "The composition of body tissues," Br. J. Radiol. **59**(708), 1209–1218 (1986).

#223215 - $15.00 USD Received 15 Sep 2014; revised 16 Oct 2014; accepted 16 Oct 2014; published 21 Oct 2014

39. J. P. Singh and S. N. Thakur, *Laser-Induced Breakdown Spectroscopy* (Elsevier Science, 2007)
40. M. Strassl, V. Wieger, D. Brodoceanu, F. Beer, A. Moritz, and E. Wintner, "Ultra-short pulse laser ablation of biological hard tissue and biocompatibles," J. Laser Micr.o Nanoengineering **3**(1), 30–40 (2008).

## 1. Introduction

Chronic inflammatory diseases and on-going mechanical stress can affect the temporo-mandibular joint (TMJ) [1, 2]. Alterations of the TMJ may lead to the deformation of the cartilaginous articular disc, the mandibular fossa or the condyles, resulting in pain and limited freedom of movement [3, 4]. While many of the therapeutic procedures specifically aim to prevent surgery on the TMJ, there are some relative and absolute indications for surgical intervention [5, 6]. The goals of surgical interventions range from the removal or shaping of diseased and altered tissues to the complete removal of joint structures, followed by insertion of disc, cartilage or condyle replacement prostheses [7]. These procedures require the selective treatment of specific articular structures. Both, minimally invasive and open surgery have been described in this context [8, 9].

Over the last years, laser surgery has developed into a generally accepted tool in various surgical specialties [10]. When compared to other standard treatment procedures such as conventional surgery using scalpels, laser surgery offers a number of advantages. The coagulation of small blood vessels allows for a dry operating field and better visibility [11–15]. Furthermore, it is possible to selectively ablate very thin tissue layers [16]. Also, laser induced wounds generally show great healing potential and are associated with less postoperative inflammation and swelling [17–21]. Bone healing showed to occur faster when compared to mechanical surgery [22]. In particular, in the field of TMJ treatment, minimally invasive surgery using an Nd:YAG has successfully been demonstrated [23]. Other authors report on successfully using a Ho:YAG-Laser for arthroscopic procedures on the TMJ [24]. One of the major drawbacks connected to surgical laser procedures is, however, the inability to definitely determine the type of tissue that is being ablated at the bottom of the cut. The actual penetration depth of the Laser is unknown. This may lead to iatrogenic damage of nerves, blood vessels or other anatomic structures that were meant to be preserved [25–28]. To overcome this limitation, the authors have previously proposed to directly use the process emissions occurring during laser surgery for a real-time identification and differentiation of the ablated tissues [29–32]. In this context, Laser Induced Breakdown Spectroscopy (LIBS) offers great potential for a laser feedback control mechanism, enabling tissue specific ablation. Using LIBS, the differentiation and identification of different soft tissues (skin, fat, muscle, nerve) has successfully been demonstrated in a previous study [29].

In this study, the focus was put on the differentiation between cartilage and cortical bone tissue. The aim was to establish the basis for a laser surgery feedback control mechanism, in order to broaden the scope of applications for clinical laser systems and to make their use safer and more efficient. To achieve the tissue differentiation, the atomic composition of the different samples was qualitatively analyzed by monitoring the plasma created during the laser ablation procedure. This was achieved by using a nanosecond-pulsed probing laser that is supposed to be used in addition to the surgical laser system.

During the deposition of a short laser pulse of sufficient energy on the surface of biological tissue, ablation of the material, followed by plasma formation, can be observed. The plasma formation results from the matrix effects initiated by the absorption of the laser energy by the ablated material [33]. When the plasma expands in the ambient air, relaxation of the plasma plume by different processes - one of which is the recombination of the free electrons with the positive ions - occurs [34]. This recombination is a radiative process which provides a continuum emission in addition to the bremsstrahlung. Another radiative process is the atomic emissions due to transitions between the different energy levels of an element from which spectrometric measurement can provide qualitative information on the atomic composition of the investigated biological samples. In addition, LIBS can also be used to provide information about the relative quantitative elemental composition of the samples. This is achieved by investigating the ratio between the intensity levels of the atomic emission

#223215 - $15.00 USD Received 15 Sep 2014; revised 16 Oct 2014; accepted 16 Oct 2014; published 21 Oct 2014
(C) 2014 OSA

lines: high concentrations of an element yield a higher intensity of the characteristic elemental emission spectra [35, 36]. In this study, the approach on the differentiation between cortical bone and cartilage was based mainly on the statistical analysis of the collected spectra. These spectra intrinsically possess the information of the different concentration levels of the elements found in both tissues. Another approach was to achieve differentiation based on the ratio between the spectral emission lines of defined elemental pairs.

## 2. Materials and methods

### *2.1 Animal model and sample preparation*

This study used sagittal bisected heads of 6 domestic pigs, 6 months of age on average. The animals were obtained from the local slaughterhouse. Therefore, approval from the ethics committee was not necessary. All animals were free of local or systemic diseases that could have altered the results. The sample preparation and experimental procedure was conducted on the day of slaughter within a maximal ex-vivo time of 6 hours. The ex-vivo time was kept within this time frame to prevent tissue alteration due to exsiccation or protein degradation.

For the cartilage samples, the hyaline cartilaginous support of the outer ear (regio helix-auriculae) was chosen. A 3x3 $cm^2$ sample was cut out using surgical scissors, the covering skin and perichondral tissue were removed mechanically using a raspatory.

The cortical bone samples were raised from the ascending branch of the mandibular bone (ramus ascendens os mandibulare). The skin and muscle tissue holding the mandible were severed using a scalpel. The whole mandibular bone, together with the condyle, was then exarticulated and cleaned from the remaining tissue, again using a raspatory. For the cortical bone samples, squares of approximately 3x3 $cm^2$ were cut out of the bone using water cooled band saw. After preparation, the samples were rinsed with sterile saline solution to remove remaining blood or tissue particles and then stored inside a sealed, opaque container at 4°C.

### *2.2 LIBS measurement setup*

The experimental setup is schematically shown in Fig. 1. The setup consisted of a frequency-doubled Nd:YAG laser (Saga Flashlamp pumped Nd:YAG Laser, Thales Group, Neuilly-Sur-Seine, France) in all of the measurements. The pulse frequency of the laser was set to 1 Hz. The pulse duration of the laser was 10 ns at a wavelength of 532 nm with average pulse energy of 80 mJ. A 100 mm focal length lens was used to focus the laser beam to a spot size of approximately 0.3 mm. A translational stage capable of moving in three dimensions was used to bring the surface of the samples to the focal spot of the laser beam. The light from the plasma generated by each laser pulse was collected by a UV-enhanced 50 µm fiber optic cable terminated with an SMA connector. The other end of the fiber was attached to a spectrometer (Mechelle ME 5000 Echelle, Andor, Belfast, UK) via another SMA connector. The spectrometer was equipped with an ICCD camera (A-DH334T-18F-03 USB iStar ICCD detector, Andor, Belfast, UK) and allowed for a spectral resolving power ($\lambda/\Delta\lambda$) of 6,000 and a measuring range of 200 – 975 nm. A digital delay generator (9618 Pulse Generator, Quantum Composers, Bozeman, USA) was used to synchronize the measurements of the detector with the laser. All the experiments were performed with a gate delay of the detector 5 µs from the laser pulse, and 1 ms gate width of the detector.

#223215 - $15.00 USD Received 15 Sep 2014; revised 16 Oct 2014; accepted 16 Oct 2014; published 21 Oct 2014
(C) 2014 OSA

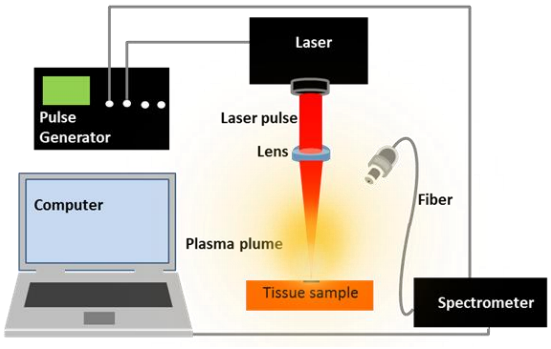


Fig. 1. Schematic of the LIBS setup used.

*2.3 LIBS measurement procedure*

The LIBS measurements were performed on each of the cartilage and cortical bone tissue samples of the 6 animals investigated. LIBS spectra were collected from 5 different spots of each sample, 5 spectra were collected from each spot. This results in a total of 150 spectra of cartilage tissue (5 spectra x 5 spots x 6 pigs) and 150 spectra of cortical bone tissue (5 spectra x 5 spots x 6 pigs). Before each measurement, 3 laser pulses were sent to the surface of each of the investigated spots. This was to remove any remaining superficial contamination of the samples, such as blood, small tissue particles or the saline solution used to clean the tissues after preparation. The ablation crater resulting from the cleaning pulses was examined under a microscope and using OCT, and it was concluded that it was deep enough to remove all of the superficial contaminants.

*2.4 Element identification and Intensity ratio analysis*

The LIBS spectra gathered from the samples were processed from the raw data using the SOLIS software (Andor, Belfast, UK). The Matlab software (Matlab R2014a, MathWorks, Natick, USA) was used for data processing. To perform the differentiation between the two tissues, first, the elements responsible for the emission at the monitored wavelengths were determined with the help of the atomic database of the National Institute of Standards and Technology (NIST, Gaithersburg, USA) [37]. For analysis purposes, only those elements which were common and prominent in the spectra of both tissue types were considered. The assignment of the elements was performed on the average spectra that represent both types of tissue. The software OriginLab (OriginLab, Northampton, USA) was used for identifying the peak wavelengths and for displaying the spectra. Then, by using the common prominent emission lines monitored in the LIBS measurements of the two tissues, three exemplary pair-wise combinations of the atomic emissions (Ca(422.67) to Na(588.99), Na(588.99) to K(766.48) and Ca(616.21) to K(766.48)) were formed to calculate ratio values. These ratio values, specific for the individual tissue type, were then compared to differentiate between the tissues.

*2.5 Statistical analysis*

The measured LIBS spectra from all the 6 animals were first normalized and mean centered. The data from 5 animals were then mixed to generate new variables with reduced dimensionality using Principal Component Analysis (PCA). The spectra from the remaining one animal were then projected on the derived variables. In this manner, PCA was performed six times by taking 5 animals to generate new fewer variables (Principal Components, PCs) by which the remaining one animal is represented. The PCA results showed that the majority of the variance in the data was contained in the first few PCs and therefore all the subsequent analyses were performed on the data represented by those. After that, Multiclass Linear Discriminant Analysis (LDA) was performed using six fold leave-one-out cross-validation on

#223215 - $15.00 USD Received 15 Sep 2014; revised 16 Oct 2014; accepted 16 Oct 2014; published 21 Oct 2014
(C) 2014 OSA

the data from the 6 animals represented by the derived variables (PCs). Each time, 5 animals were taken as the training data and the remaining one animal as the sample data. This resulted in a prediction of class membership of the tissues of each animal. The prediction performance of the classifier was then evaluated using Receiver Operating Characteristic (ROC). The Area under the ROC curve (AUC) of the investigated tissue pair of all the animals was computed. Additionally, the values of the sensitivity and specificity at the cut–off point of the tissue pair of each animal were calculated. Computation of PCA, LDA and ROC analysis was performed using the Matlab statistical tool box.

## 3. Results and discussion

To exemplify, the mean spectra (Mean Value and Standard Deviation) of 25 cartilage spectra and 25 bone-spectra of animal #1 are shown in Fig. 2. Spectral analysis of the other animals yielded similar results. To exemplify, the most prominent peaks existing in the spectra of both tissue samples were used to show the standard deviation of all of the 50 spot-measurements (5 Spectra x5 Spots x 2 Tissues) of animal #1 (Fig. 2). The elements and a molecule with prominent emissions common to both tissue types, found under the measurement conditions of this study, were Ca, Na, K and CN (Fig. 2). Already, a difference in wavelength-associated intensity values between bone and cartilage tissue can be observed.

The LIBS spectra of cortical bone exhibit more prominent atomic spectral lines than those of cartilage. This may be owed to the higher concentration of the elements in bone than in cartilage [38]. LIBS measurements of the two different tissues yielded similar tissue specific results in all of the investigated animals. Similar spectral features within tissues of one class but different features between classes were successfully demonstrated. This indicates that the concentration of the elements responsible for the emissions at the monitored peaks is different in the two classes of tissues.

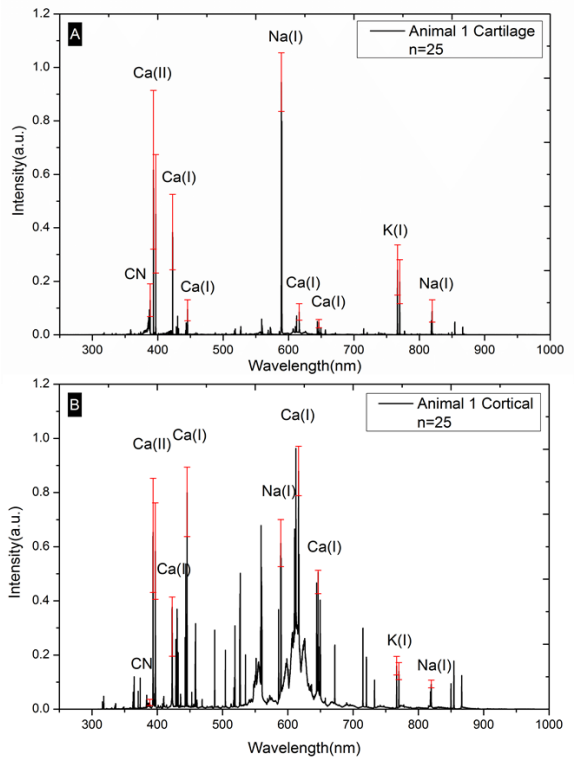


Fig. 2. (A) Mean LIBS spectra of cartilage of animal #1. (B) Mean LIBS spectra of cortical bone of animal #1.

#223215 - $15.00 USD Received 15 Sep 2014; revised 16 Oct 2014; accepted 16 Oct 2014; published 21 Oct 2014
(C) 2014 OSA

When comparing the LIBS spectra of cortical bone and cartilage, the spectra collected from the bone samples were observed to have much more prominent atomic spectral lines under the conditions of the experiments. This may result from the higher number of excited atoms due to the higher density of cortical bone [33, 39]. Based on the results obtained, three approaches may be taken to perform the differentiation: based on unique emission lines in the spectrum of cortical bone; based on the ratio values calculated from the intensity level of the atomic spectral lines that are common to both tissue types; or based on statistical analysis techniques. However, the use of unique emission lines can be an unstable approach when higher excitation energies are used. Higher excitation energies may provide spectra with common emission lines differing only in intensity levels as the qualitative elemental composition of the two tissues is similar. Calculation of the ratio values among the emission lines and statistical analysis techniques were attempted to differentiate between both tissue types.

### *3.1 Intensity ratio analysis*

One approach to differentiate the tissues is to calculate intensity ratio values between different pairs of emission lines, as described above. To generate ratio features from the spectra, emissions from Ca, Na and K at the selected wavelengths (Fig. 2) were used. The choice of Ca emissions for ratio analysis was mainly owed to its high concentration in the tissue samples. This may help to detect the element regardless of the highly heterogeneous nature of the tissues which resulted in the variation of the intensity of the spectra. The choice of Na and K peaks and their wavelength is mainly due to their higher intensity values to facilitate the visualization and discussion of the results. However, it should be noted that the spectra obtained in this study are rich in information and many other ratio features from other elements with low intensity values can be generated.

Many different combinations of ratios can be established using the emissions of the selected three elements. For discussion purposes, three pairs of emissions will be considered for ratio analysis (Ca(422.67) to Na(588.99), Na(588.99) to K(766.48) and Ca(616.21) to K(766.48)). The results of ratio values calculated from the emission intensities of the pairs are shown in Fig. 3. The ratio between the intensity levels of Ca(616.21) to K(766.48) can be seen to differentiate the tissues very well. This ratio showed to consistently produce values less than one in cartilage and greater than one in bone (Fig. 3). As already mentioned, several other ratio combinations from the measured spectra may be considered to differentiate between the two tissue types. Although analyzing the spectra using the ratio of the intensity of emissions can provide a very good differentiation results, focus is laid on statistical analysis techniques in order to make use of the difference in the spectra along the entire wavelength range investigated.

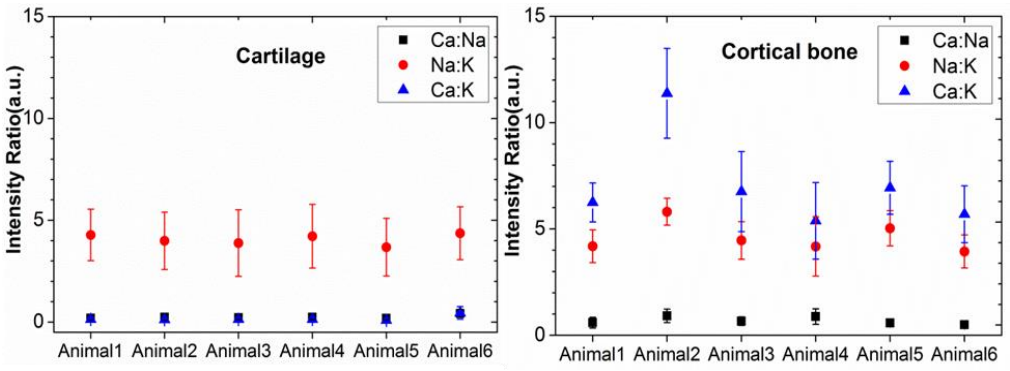


Fig. 3. Intensity ratio values of cartilage and cortical bone calculated from three pairs of atomic emission lines. (Black) Ca(422.67) to Na(588.99), (Red) Na(588.99) to K(766.48) and (Blue) Ca(616.21) to K(766.48)).

#223215 - $15.00 USD Received 15 Sep 2014; revised 16 Oct 2014; accepted 16 Oct 2014; published 21 Oct 2014
(C) 2014 OSA

*3.2 Statistical analysis*

To reduce the high dimensionality nature of the data, PCA was used to derive new variables (PCs) using the original spectra represented by intensities in the investigated wavelength range. The establishment of PCs was performed based on the data of 5 animals. An example of PCA analysis on animals # 1 – #5 is shown in Fig. 4. The results of these 5 animals show a clear separation of the two tissue classes, see Fig. 4(A). The ability of the PCs to separate the two classes can however be best evaluated by projecting on the PCs the measurements from a separate animal which was not used when deriving the PCs. This is shown in Fig. 4(B) where the data from animal #6 is projected on the PCs shown in Fig. 4(A). The figure shows that the PCs separate the tissues consistently based on their type. In this manner, each animal was used as a verification data for the PCs derived from the other 5 animals (six different groups were investigated). Clear separation of the two classes could be seen in all the results. The results of PCA on the six different groups of the animals shows almost all the variance (more than 99.5%) of the data is contained in the first 10 PCs. Table 1 shows the details of the portions of the variance contained in each of the PCs of the different groupings of the 6 animals. An average of 84.59% of the total variance accounts for by PC1. PC2 represents an average of 10.57%, PC3 an average of 2.46% of the total variance. The remaining portion of the 99.5% was contained in PC4 – PC10. Therefore, the high dimensionality nature of the data was reduced to only 10 PCs by ignoring the remaining PCs containing less than 0.5% of the total variance. The results of PCA representing the data of each animal in terms of new variables were used to perform classification analysis using LDA.

**Table 1. Portion of variance covered by the PCs on the total variance of the LIBS spectra.**

| Animal Group | PC1 | PC2 | PC3 | PC4 | PC5 | PC6 | PC7 | PC8 | PC9 | PC10 | Total |
|---|---|---|---|---|---|---|---|---|---|---|---|
| **1,2,3,4,5** | .8379 | .1153 | .0240 | .0070 | .0042 | .0027 | .0021 | 0.0011 | .0007 | .0005 | .9954 |
| **1,2,3,4,6** | .8655 | .0870 | .0240 | .0060 | .0048 | .0035 | .0024 | 0.0011 | .0007 | .0005 | .9954 |
| **1,2,3,5,6** | .8454 | .1063 | .0244 | .0067 | .0046 | .0035 | .0023 | 0.0009 | .0008 | .0006 | .9956 |
| **1,2,4,5,6** | .8443 | .1106 | .0224 | .0061 | .0042 | .0033 | .0024 | 0.0011 | .0008 | .0005 | .9956 |
| **1,3,4,5,6** | .8291 | .1186 | .0278 | .0074 | .0050 | .0027 | .0022 | 0.0011 | .0009 | .0006 | .9953 |
| **2,3,4,5,6** | .8532 | .0964 | .0251 | .0060 | .0054 | .0040 | .0027 | 0.0012 | .0007 | .0006 | .9953 |

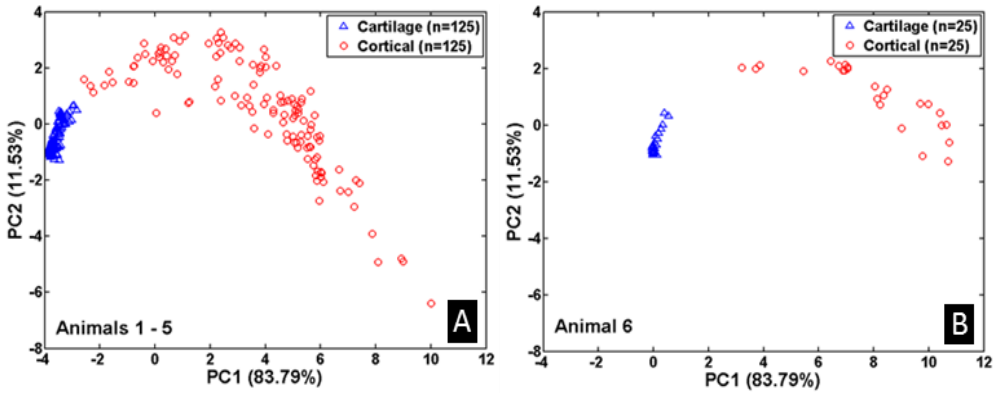


Fig. 4. (A) PCA of animal #1 - #5. (B) Projection of animal #6 on PCs of animal #1 - #5.

Table 2 shows the confusion matrices resulting from the LDA classification analysis, used to predict the class membership of the measurements using six fold leave-one-out cross-validation. As shown in Table 2, high classification performance was achieved in the analysis

#223215 - $15.00 USD Received 15 Sep 2014; revised 16 Oct 2014; accepted 16 Oct 2014; published 21 Oct 2014
(C) 2014 OSA

of each of the 6 animals. The misclassification error was zero in all the classification results. The classifier could accurately differentiate all the measurements of cartilage of each animal from the corresponding cortical bone measurements. The performance of the classifier was further evaluated by ROC analysis.

**Table 2. Confusion Matrices of the classification result of cartilage and cortical bone of six animals.**

| **Animal 1** | **Cartilage** | **Cortical** | **Animal 2** | **Cartilage** | **Cortical** |
|---|---|---|---|---|---|
| **Cartilage** | 25 | 0 | **Cartilage** | 25 | 0 |
| **Cortical** | 0 | 25 | **Cortical** | 0 | 25 |
| **Animal 3** | **Cartilage** | **Cortical** | **Animal 4** | **Cartilage** | **Cortical** |
| **Cartilage** | 25 | 0 | **Cartilage** | 25 | 0 |
| **Cortical** | 0 | 25 | **Cortical** | 0 | 25 |
| **Animal 5** | **Cartilage** | **Cortical** | **Animal 6** | **Cartilage** | **Cortical** |
| **Cartilage** | **25** | **0** | **Cartilage** | 25 | 0 |
| **Cortical** | **0** | **25** | **Cortical** | 0 | 25 |

The ROC analysis results from all the six animals also shows high classification performance of the classifier. The value of the area under the ROC curve (AUC) of each animal was 1.00. Table 3 shows the values of AUC of all the investigated animals. Figure 5 shows an exemplary ROC curve obtained from the classification result of animal #6. Similar ROC curves were also obtained from the classification results of the remaining 5 animals. Therefore, the ROC analysis confirmed the high classification performance of the classifier.

**Table 3. Area under the ROC (AUC) curve values of cartilage and cortical bone classification of 6 animals.**

| **Animal 1 AUC** | **Animal 2 AUC** | **Animal 3 AUC** | **Animal 4 AUC** | **Animal 5 AUC** | **Animal 6 AUC** |
|---|---|---|---|---|---|
| 1.00 | 1.00 | 1.00 | 1.00 | 1.00 | 1.00 |

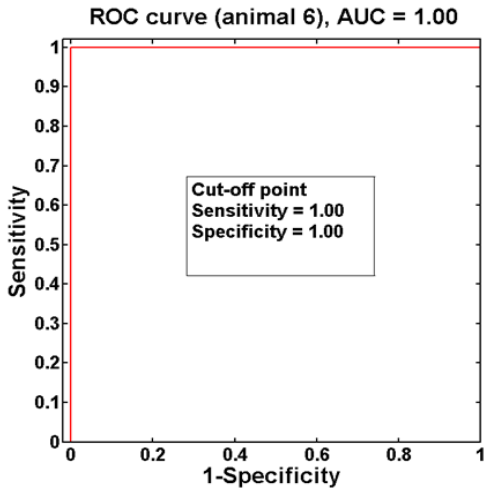


Fig. 5. ROC curve of animal #6.

**Table 4. Sensitivity and specificity values of 6 animals.**

| | **Sensitivity** | **Specificity** | | **Sensitivity** | **Specificity** |
|---|---|---|---|---|---|
| **Animal 1** | 1.00 | 1.00 | **Animal 4** | 1.00 | 1.00 |
| **Animal 2** | 1.00 | 1.00 | **Animal 5** | 1.00 | 1.00 |
| **Animal 3** | 1.00 | 1.00 | **Animal 6** | 1.00 | 1.00 |

#223215 - $15.00 USD Received 15 Sep 2014; revised 16 Oct 2014; accepted 16 Oct 2014; published 21 Oct 2014
(C) 2014 OSA

The sensitivity and specificity values of all the animals were calculated at the optimum cut-off point (Table 4). In all the analyses 100% sensitivity and specificity were achieved. This again confirms the clear differentiation of cartilage from bone with very high accuracy.

In the measured spectra from the two tissues, several spectral feature differences were observed. This may be owed to the significant difference in the physical characteristics of the samples, mainly in terms of density and surface topology. Variations of plasma volume, temperature and electron density always result in shot-to-shot variations of both the absolute and relative intensities of spectral lines, which results in poor reproducibility of the spectra [33, 39]. In this study, the substantially different physical characteristics of the investigated tissues may, however, have negated the effect of shot-to-shot variations on the differentiation performance. Therefore, the investigated tissues can be differentiated using the technique on a pulse-to-pulse basis without the need for spectral averaging. Depending on the speed and extent of ablation caused by the surgical Laser system, in-vivo experiments will have to show whether continuous pulse-to-pulse measurement is really necessary, or if timed sampling in predefined intervals is sufficient for the clinical implementation of a feedback system.

### *3.3 Technical and medical considerations*

This study used sagittal separated pig heads as an animal model for the experiments. The results may not be directly comparable to those found in humans. Additionally, the fact that ex-vivo material was used might have had an influence on the observed data, although the ex-vivo time was kept as short as possible. Tissue degeneration, protein degradation, exsiccation and the lack of blood perfusion may have altered the measured spectra. The measurements were performed on cartilage tissue from the auricle. Using the articular disc was not possible. The young (6 months of age) animal's discs were, upon preparation, found to be very thin and fragile. Isolation would have been associated with major structural mechanical damage and a clear visual differentiation between connective tissue and cartilaginous articular disc was not possible. The cartilage found in the auricle is of the hyaline sort and that of the articular disc is fibrocartilaginous. Both tissue variants share the same basic structure, examination of the fibrocartilaginous articular disc may however yield different results.

As previously assumed by Strassl et al. [40], discrimination between the two tissue types was possible. Performing statistical analysis techniques, PCA followed by LDA, on the atomic emission spectra measured from the plasma created during laser ablation allowed for highly accurate differentiation. Using the less complicated ratio comparison approach yielded equally significant differentiation performance. The demonstrated technique could be an excellent candidate for the development of a real-time feedback control mechanism that prevents the unwanted removal of cortical bone or cartilage tissue during laser based surgical procedures. One of the future goals derived from this study is to extensively investigate the ablation thresholds and ablation rates of the tissues to minimize possible collateral damage caused by the lasers. Different Laser systems and experimental parameters should be investigated taking into account both technical and medical aspects. This may help to broaden the field of application of surgical laser systems and make their use more robust and safer; a future application in the field of TMJ-surgery is imaginable.

## 4. Conclusion

This study successfully demonstrated the LIBS-based differentiation between porcine ex-vivo cartilage and cortical bone tissue using PCA for feature extraction and performing LDA for the prediction of the class membership. Classification results that enable the differentiation of the investigated samples with 100% sensitivity and 100% specificity are achieved. Furthermore, equally effective differentiation by emission-intensity-ratio comparison between specific atomic emission lines was demonstrated. This suggests that LIBS can provide real-time qualitative information about the atomic composition of a processed sample. However, it should be noted that in a clinical setting, the investigated tissues may also need to be identified from other surrounding soft tissues. These surrounding tissues may not show usable atomic emissions like those considered for ratio analysis in this study. Therefore, the use of

#223215 - $15.00 USD Received 15 Sep 2014; revised 16 Oct 2014; accepted 16 Oct 2014; published 21 Oct 2014
(C) 2014 OSA

statistical analysis may be more feasible and certainly more accurate when including unknown parameters, such as other tissues, in the analysis. Moreover, it should be noted that the experiments were performed on ex-vivo tissue samples. Further in-vivo studies will have to demonstrate if these results are reproducible.

**Acknowledgment**

The authors gratefully acknowledge the funding of the Erlangen Graduate School in Advanced Optical Technologies (SAOT) by the Deutsche Forschungsgemeinschaft (German Research Foundation - DFG) within the framework of the Initiative for Excellence.

#223215 - $15.00 USD Received 15 Sep 2014; revised 16 Oct 2014; accepted 16 Oct 2014; published 21 Oct 2014